Inorg. Chem. **2006**, *45*, 10728–10733

La_2TeI_2: A New Layered Telluride Iodide with Unusual Electrical Properties

Mikhail Ryazanov, Arndt Simon,* and HansJürgen Mattausch

Max-Planck Institut für Festkörperforschung, Heisenbergstrasse 1, D-70569 Stuttgart, Germany

Received September 5, 2006

A new layered metal-rich telluride halide, La_2TeI_2, has been synthesized by heating stoichiometric mixtures of LaI_3, La, and Te under argon at 900 °C, and its structure has been refined from X-ray powder diffraction data. The compound crystallizes in the 3R-Lu_2CCl_2 structure type (rhombohedral space group $R\bar{3}m$ with $a = 4.5074(4)$ Å, $c = 32.528(2)$ Å, and $Z = 3$). The crystal structure is composed of infinite layers of edge-sharing, Te-centered metal atom octahedra and iodine atoms separating these layers to form three close-packed I–Ln–Te–Ln–I slabs within the unit cell. The title compound is metallic at room temperature and exhibits an anomaly in the resistivity around 140 K which is closely related to changes in the *a* lattice parameter with temperature. The chemical bonding and metallic properties of La_2TeI_2 can be plausibly understood in terms of an ionic description $(Ln^{3+})_2Te^{2-}(I^-)_2(e)_2$ where two electrons are delocalized in the La 5d conduction band.

Introduction

The zirconium monohalides ZrCl[1] and ZrBr[2] and ternary M_2ZX_2 halides (X = Cl, Br, or I) of Zr[3,4] and the trivalent rare-earth elements with interstitial nonmetal atoms, Z, constitute a closely related family of layered compounds. They all feature infinite close-packed bilayers of metal atoms that are sandwiched by layers of halogen atoms, forming cubic closed-packed stacking sequences X−M−M−X. Such slabs are in turn bound with each other by weak van der Waals forces with the translation period varying from three slabs per unit cell as in ZrCl,[1] ZrBr,[2] and the so-called 3R structures of M_2ZX_2[3,5] to only one slab as in the 1T structures of M_2ZX_2.[3,5,6] In the ZrX phases, three electrons per metal contribute to the robust bonding within the metal atom double layers and the compounds are two-dimensional metallic systems. On the other hand, for the more electron deficient rare earth metals, interstitial species are required to stabilize the structure by introducing strong metal−interstitial interactions. A variety of such interstitial phases are known for Sc, Y, and lanthanide halides, mostly chlorides and bromides, with the endohedral units Z including H,[7,8] N,[3] O,[9] C (single atoms[3,5,6] or C_2 units[6,10]), and Ge.[11] Normally, nitrogen and oxygen atoms occupy the tetrahedral voids between metal atoms, whereas the larger carbon and germanium atoms prefer octahedral voids. Hydrogen atoms can reside in tetrahedral voids[7,8] or near to the parallel faces of trigonal antiprisms,[4] or in both, as found for $M_2H_4X_2$.[8]

In addition to their peculiar chemical and structural features, the M_2ZX_2 phases exhibit striking physical properties associated with low-dimensional strongly correlated electron systems. Therefore, the metallic $M_2C_2X_2$ (M = Y, La; X = Cl, Br, or I) carbide halides are low-temperature superconductors with the maximum transition temperature reaching $T_c = 11.6$ K.[12] The nonstoichiometric YH_xI phases

* To whom correspondence should be addressed. E-mail: a.simon@fkf.mpg.de.

(1) Izmailovich, A. S.; Troyanov, S. I.; Tsirelnikov, V. I. *Russ. J. Inorg. Chem.* **1974**, *19*, 1597. Adolphson, D. G.; Corbett, J. D. *Inorg. Chem.* **1976**, *15*, 1820.
(2) Daake, R. L.; Corbett, J. D. *Inorg. Chem.* **1977**, *16*, 2029.
(3) Hwu, S.-J.; Ziebarth, R. P.; Winbush, S. v.; Ford, J. E.; Corbett, J. D. *Inorg. Chem.* **1986**, *25*, 283.
(4) Wijeyesekera, S. D.; Corbett, J. D. *Solid State Commun.* **1985**, *54*, 657.
(5) Schleid, T.; Meyer, G. *Z. Anorg. Allg. Chem.* **1987**, *552*, 90.
(6) Schwanitz-Schüller, U.; Simon, A. *Z. Naturforsch.* **1985**, *B40*, 710.
(7) Ueno, F.; Ziebeck, K.; Mattausch, H.; Simon, A. *Rev. Chim. Miner.* **1984**, *21*, 804. Meyer, G.; Hwu, S.-J.; Wijeyesekera, S. D.; Corbett, J. D. *Inorg. Chem.* **1986**, *25*, 4811. Cockcroft, J. K.; Bauhofer, W.; Mattausch, H.; Simon, A. *J. Less-Common Met.* **1989**, *152*, 227.
(8) Mattausch, H.; Simon, A.; Ziebeck, K. *J. Less-Common Met.* **1985**, *113*, 149. Mattausch, H.; Schramm, W.; Eger, R.; Simon, A. *Z. Anorg. Allg. Chem.* **1985**, *530*, 43. Mattausch, H.; Eger, R.; Corbett, J. D.; Simon, A. *Z. Anorg. Allg. Chem.* **1992**, *616*, 157. Ryazanov, M.; Simon, A.; Mattausch, H. *Z. Anorg. Allg. Chem.* **2004**, *630*, 1401.
(9) Ford, J. E.; Corbett, J. D. *Inorg. Chem.* **1985**, *24*, 4120.
(10) Schwarz, C.; Simon, A. *Z. Naturforsch.* **1987**, *B42*, 935.
(11) Mattausch, H.; Zheng, C.; Ryazanov, M.; Simon A. *Z. Anorg. Allg. Chem.* **2005**, *631*, 302.

10.1021/ic061675r CCC: $33.50
Published on Web 11/17/2006

undergo a continuous transition from an itinerant to a localized electronic state at low temperatures,[13] whereas the magnetic analogues GdH_xI exhibit a colossal negative magnetoresistance as large as 3 orders of magnitude at 2 K for $x \approx 0.7$.[13,14]

Recently we succeeded in preparing layered telluride halides Ln_2TeI_2 (Ln = La, Gd), which are the first members of the M_2ZX_2-type compounds with tellurium atoms acting as interstitials. To the best of our knowledge, only one example of Te-containing ternary rare earth halides is known so far. This is a nonstoichiometric $Er_{17.3}Te_{24}I_8$ phase that adopts a three-dimensional structure with polycationic and polyanionic fragments, derived from the cubic rocksalt type.[15] Here we report the synthesis, crystal structure and electrical properties of La_2TeI_2, which exhibits a resistivity anomaly characteristic of a charge density wave (CDW) instability. The results of first principles electronic structure calculations for La_2TeI_2 are also reported.

Experimental Section

Synthesis. All compounds were handled under purified Ar either in a glovebox (H_2O < 0.2 ppm; O_2 < 0.8 ppm) or by employing standard Schlenk techniques. La metal pieces (99.99%; Johnson Matthey, Germany), LaI_3, Te (99.999%; Aldrich), and iodine powder (99.8%; Merck) were utilized as starting materials. LaI_3 was prepared from the elements in an evacuated sealed silica tube by slowly heating from 300 to 900 °C and further purified by two subsequent sublimations at 930 °C in high vacuum (10^{-4} Torr).

La_2TeI_2 was synthesized by solid-state reaction of the starting materials (LaI_3/La/Te = 2:4:3) at 900 °C for 6 days. The reaction mixture (ca. 1 g) was ground, pressed into a pellet, and then heated in an arc-welded Ta ampule filled with argon. To prevent oxidation of the container, the Ta tube was further sealed in an evacuated silica jacket. After reaction, the ampule was cooled to room temperature at a rate of 10 °C/h. The product, observed under the microscope, contained a dark bronze colored microcrystalline powder composed of thin golden platelets and a small amount of bulky violet crystals which had been identified as LaTe. According to the X-ray powder diffraction patterns, the content of the binary phase amounted to ~5−10 wt % (after Rietveld analysis). The compounds obtained are very reactive with air, resulting in strongly smelling oxidized or hydrolyzed products. EDX (energy dispersive X-ray spectroscopy) analyses of thin plate crystals, using a Tescan scanning electron microscope equipped with an Oxford EDX detector, confirmed the presence of La,Te, and I elements in an atomic ratio of 2:1:2 (standard deviation <5 %). A number of La_2TeI_2 crystals (~30 mg) were mechanically separated under the microscope and used for further studies.

Powder X-ray Analysis. The isolated samples of La_2TeI_2 were mixed with some glass powder and sealed in glass capillaries (diameter: 0.2 mm) filled with Ar. X-ray diffraction patterns were recorded in Debye−Scherrer geometry on a Stoe Stadi P diffractometer (Mo K_α radiation, $\lambda = 0.7093$ Å, germanium monochromator). Low-temperature XRD experiments were performed on the same instrument equipped with a self-constructed cooling system, the operating temperature range being between 100 and 300 K. Lattice dimensions and atomic parameters were refined by Rietveld analysis using the FullProf program.[16] The pseudo-Voigt function was used for simulation of the peak shapes. All reflections were corrected for asymmetry (2θ < 40°) and preferred orientation effects using the March−Dollase function.[17] Figure 1 shows the final Rietveld refinement pattern for a selected La_2TeI_2 sample used for further physical measurements. According to the results of a detailed pattern matching, the sample contained a minor amount of the secondary-phase LaTe (ca. 2%). Crystallographic data for La_2TeI_2

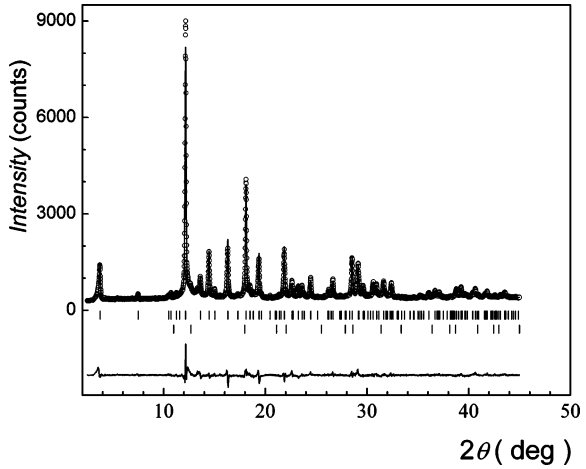

Figure 1. X-ray powder diffraction pattern for La_2TeI_2 taken at 293 K. The observed pattern is denoted by "○"; the solid line corresponds to the best Rietveld fit profile; vertical bars indicate the calculated reflection positions for La_2TeI_2 (top) and LaTe (bottom). The bottom trace represents the difference between observed and calculated profiles.

Table 1. Selected Data from the Structure Rietveld Refinement of La_2TeI_2

fw	659.22	
cryst syst	trigonal	
space group	$R\bar{3}m$ (No. 166)	
temp (K)	293(2)	120(1)
wavelength (Å)	0.7093 (Mo K_α)	
lattice dimensions (Å)		
a	4.5074(4)	4.4981(5)
c	32.528(2)	32.402(3)
V (Å^3), *Z*	572.3(2), 3	567.8(2), 3
ρ_{calc} (g•cm^{-3})	5.74	5.78
μ (cm^{-1})	227.6	229.4
scan range	2.5° < 2θ < 45.0°	
no. of collected points (*N*)	4250	4250
no. of reflns	148	152
no. of refined params (*P*)	15	15
correction for preferred orientation	March−Dollase function	
	$G_1 = 1.079(3)$	$G_1 = 1.114(3)$
final *R* indices[a] R_p	0.084	0.098
R_{wp}	0.109	0.128
R_{exp}	0.059	0.066
R_B	0.089	0.091
GOF[b]	1.85	1.94

[a] $R_p = \sum_{i=1,N}|y_i - y_{c,i}|/\sum_{i=1,N}y_i$, $R_{wp} = [\sum_{i=1,N}w_i|y_i - y_{c,i}|^2/\sum_{i=1,N}w y_i^2\}]^{1/2}$, $R_{exp} = [(N - P)/\sum_{i=1,N}wy_i^2]^{1/2}$, $R_B = \sum_i|I_{obs,i} - I_{calc,i}|/\sum_i|I_{obs,i}|$. [b] GOF = R_{wp}/R_{exp}.

(12) Simon, A.; Mattausch, H.; Eger, R.; Kremer, R. K. *Angew. Chem.* **1991**, *103*, 1209. *Angew. Chem., Int. Ed. Engl.* **1991**, *30*, 1188. Simon, A.; Yoshiasa, A.; Bäcker, M.; Henn, R. W.; Felser, C.; Kremer, R. K.; Mattausch, H. *Z. Anorg. Allg. Chem.* **1996**, *622*, 123. Henn, R. W.; Schnelle, W.; Kremer, R. K.; Simon, A. *Phys. Rev. Lett.* **1996**, *77*, 374.
(13) Ryazanov, M.; Kremer, R. K.; Simon, A.; Mattausch, H. *Phys. Rev. B* **2006**, *73*, 0351141.
(14) Bauhofer, W.; Joss, W.; Kremer, R. K.; Mattausch, H.; Simon, A. *J. Magn. Magn. Mater.* **1992**, *104−107*, 1243.
(15) Stöwe, K. *J. Solid State Chem.* **1998**, *139*, *57*.
(16) Rodriguez-Carvajal, J. *FullProf 2k Version 2.50*; LLB CEA-CNRS: Gif sur Yvette, France, 2003.
(17) Dollase, W. A. *J. Appl. Crystallogr.* **1986**, *19*, 267.

Table 2. Atomic Coordinates and Equivalent Isotropic Displacement Parameters ($Å^2 \times 10^3$) for La_2TeI_2 at 293 and 120 K (Given in Square Brackets)

atom	*x/a*	*y/b*	*z/c*	U_{eq}
La	0	0	0.1120(1)	32(1)
			[0.1119(1)]	[31(1)]
I	0	0	0.2827(1)	38(1)
			[0.2828(1)]	[37(1)]
Te	0	0	1/2	30(1)
				[28(1)]

Table 3. Selected bond distances (Å) in La_2I_2Te at 293 and 120 K (Given in Square Brackets)

La−La	4.507(1)	I−I	4.507(1)
	[4.498(1)]		[4.498(1)]
	4.407(4)[a]		4.198(4)[a]
	[4.396(3)][a]		[4.178(3)][a]
La−I	3.280(3)	Te−Te	4.507(1)
	[3.272(2)]		[4.498(1)]
La−Te	3.152(2)	I−Te	4.585(3)
	[3.144(2)]		[4.573(2)]

[a] Interlayer distances.

are summarized in Table 1. The atomic positions and isotropic displacement parameters are listed in Table 2; Table 3 presents important interatomic distances in the structure.

Electronic Structure Calculations. First-principles DFT band structure calculations for LaI were carried out in the local density approximation using the Stuttgart TB-LMTO program.[18,19] The eigenvalue problem was solved on the basis of the von Barth−Hedin local exchange−correlation potential[20] taking all relativistic effects into account except for the spin−orbit coupling. The *k* space integration was performed using the tetrahedron method[21] with 781 irreducible points within the rhombohedral Brillouin zone. Further computational parameters are given in the Supporting Information. In addition, a study of the crystal orbital Hamiltonian population (COHP)[22] was performed to get a better insight into the chemical bonding of La_2TeI_2.

Physical Properties. Electrical resistance, *R*, was determined on pressed-powder pellets of 3 mm diameter (thickness $h \approx 0.5$ mm) by the van der Pauw method[23] in a temperature range of 10−290 K. The samples were connected to gold wire contacts of a four-point probe setup using commercial silver paste (Epo-Tek H20E, Polytec, Germany). Each $R(T)$ curve was recorded both in cooling and heating modes by measuring the voltage when a constant current of 1 mA was applied. To approximately evaluate the resistivity values, we used the van der Pauw formula $\rho\ (\Omega\cdot\text{cm}) \approx R(\Omega)\ h(\text{cm})\ \pi/\ln 2$.

Magnetization measurements were performed with a SQUID magnetometer (MPMS, Quantum Design, 6325 Lusk Boulevard, San Diego) between 2 and 350 K in dc magnetic fields $H = 1$, 3, and 5 T. A polycrystalline sample of about 40 mg was pressed into a pellet and sealed in a silica ampule under 1 atm He exchange gas to provide sufficient thermal contact. The magnetic data were corrected for the sample holder contribution and for the diamagnetism of the constituent atoms estimated from Pascal's increments (La^{3+}, -20×10^{-6} cm³/mol; I^-, Te^{2-}, -52×10^{-6} cm³/mol).[24,25]

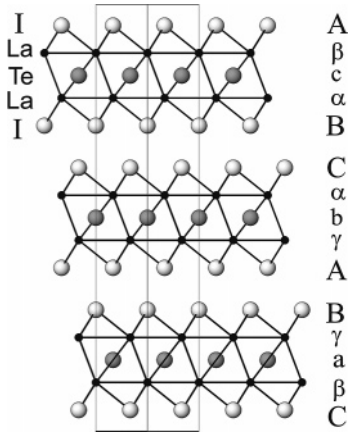

Figure 2. Projection of the structure of La_2TeI_2 along [110]. The stacking sequence of close-packed layers within the unit cell is shown in the ABC notation.

Results and Discussion

Structural and Physical Properties. La_2TeI_2 crystallizes in the rhombohedral 3R-Lu_2CCl_2-type structure[5] with lattice dimensions of $a = 4.5074(4)$ Å and $c = 32.528(2)$ Å. The arrangement of atoms has been refined from X-ray powder diffraction data by the conventional Rietveld method.[26] The crystal structure is built from planar layers of edge-sharing, Te-centered octahedra of the metal atoms and I atoms separating these layers to form three closed-packed I−Ln−Te−Ln−I slabs within the unit cell (Figure 2). Along the *c* direction, these slabs are bound to each other via van der Waals interactions in the stacking sequence AβcαB CαbγA BγaβC. The closest I−I contact between adjacent I−Ln−Te−Ln−I slabs is equal to 4.19 Å. Due to the rather identical scattering cross sections of Te^{2-} and I^-, some statistical distribution of the anions cannot be ruled out; however, this seems improbable, as there is no sign of a range of homogeneity.[27] It is interesting to note that when neglecting the distinction between tellurium and iodine atoms, which are actually indistinguishable by X-ray diffraction methods, the arrangement in a single La_2TeI_2 slab corresponds to that of the A-form of the rare-earth sesquioxides Ln_2O_3.[28] In this case, the structure of La_2TeI_2 can be described as a cubic close-packed sequence of A-Ln_2O_3-type blocks.

The shortest La−La distance is 4.41 Å between adjacent metal atom layers. The intralayer distance between La atoms (4.51 Å) is somewhat longer than the interlayer one, indicating weaker bonding M−M interactions within a single

(18) Andersen, O. K.; Jepsen, O. *Phys. Rev. Lett.* **1984**, *53*, 2571.
(19) Tank, R. W.; Jepsen, O.; Burkhardt, A; Andersen, O. K. *TB-LMTO-ASA 4.7*; Max-Planck Institut für Festkörperforschung: Stuttgart, Germany, 1998.
(20) von Barth, U.; Hedin, L. *J. Phys. C* **1972**, *5*, 1629.
(21) Blöchl, P. E.; Jepsen, O.; Andersen, O. K. *Phys. Rev. B* **1994**, *49*, 16223.
(22) Dronskowski, R.; Blöchl, P. E. *J. Phys. Chem.* **1993**, *97*, 8617.
(23) van der Pauw, L. J. *Philips Res. Rep.* **1958**, *13*, 1−9.
(24) Carlin, R. L. *Magnetochemistry*; Springer-Verlag: Berlin, Heidelberg, New York, Tokyo, 1986.
(25) The diamagnetic Pascal increments for isoelectronic I^- and Te^{2-} closed-shell ions were assumed to be almost identical.
(26) Rietveld, H. M. *J. Appl. Crystallogr.* **1969**, *2*, 65.
(27) Attempts to synthesize mixed $La(I_{1-x}Te_x)_2$ compounds by heating appropriate mixtures of LaI_2 and $LaTe_2$ at 820 °C resulted in the formation of stoichiometric binary and ternary phases: La_2TeI_2/La_2I_5 ($x = 0.1$), $LaI_3/LaTe$ ($x = 0.2$), or LaI_3/La_2Te_3 ($x = 0.5$).
(28) Aldebert, A.; Traverse, J. P. *Mater. Res. Bull.* **1979**, *14*, 303.

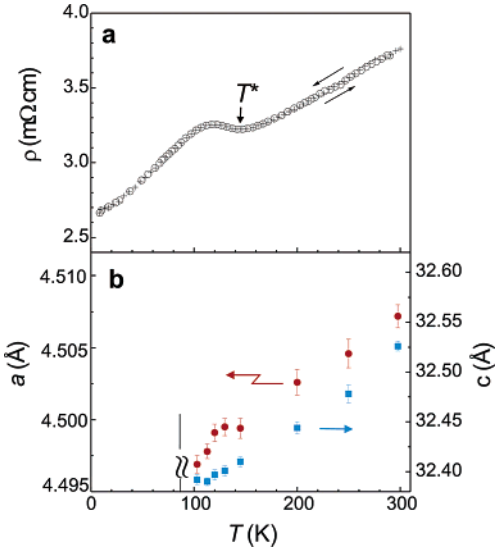

Figure 3. (a) Temperature dependence of the electrical resistivity, ρ, for La_2TeI_2, measured both in cooling and heating modes. T^* represents the onset temperature of a resistivity/structural transition. (b) Variation of the lattice parameters of La_2TeI_2 with temperature.

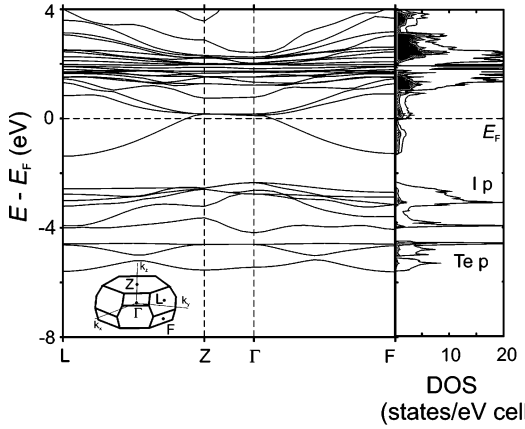

Figure 4. LMTO band structure and electronic densities of states (DOS) of La_2TeI_2 with partial contributions of lanthanum 5d states (filled area). The inset shows the Brillouin zone for a rhombohedral structure with special k points outlined. The dashed line marks the Fermi level.

layer. According to Pauling's concept of bond order,[29] the observed La−La distances of 4.41 and 4.51 Å correspond to a metallic bond order of 0.019 (×3) and 0.013 (×6), respectively. The La−I bond length is equal to 3.28 Å, which is slightly larger than the sum of ionic radii (La^{3+}, 1.03; I^-, 2.20 Å). On the other hand, the La−Te distances within the La_6Te units (3.15 Å) are 0.09 Å shorter than those expected for pure ionic bonding. The bond distance relations in La_2TeI_2 can thus be plausibly understood in terms of an ionic description, $(Ln^{3+})_2Te^{2-}(I^-)_2(e^-)_2$, taking into account enhanced cation−anion attraction effects through the highly charged Te^{2-} ions. The excess valence electrons contribute to metal−metal bonding, thus implying metallic conductivity for the title compound.

Figure 3a shows the temperature dependence of the electrical resistivity for La_2TeI_2. The sample exhibits indeed metallic behavior with a positive slope $d\rho/dT$. The resistivity is ∼3.7 mΩ·cm at room temperature and decreases linearly when the temperature is lowered to 200 K. However, at lower temperatures, ρ shows a broad humplike feature near $T^* =$ 140 K before reaching values of 2.6 mΩ·cm at 10 K. A similar resistivity anomaly has been observed in layered transition metal chalcogenides and bronzes with nested Fermi surfaces.[30,31] Such compounds have a tendency to lower their electronic energy by undergoing a periodic lattice distortion, causing a structural transition due to induced modulation of the electronic density at the Fermi level (Charge Density Wave instability).

The most remarkable feature is that the a lattice parameter of La_2TeI_2 as a function of temperature shows the same humplike feature as found in $\rho(T)$, whereas the c parameter changes monotonically with decreasing temperature (see Figure 3b). This indicates that the observed resistivity anomaly is closely related to the variation in atomic distances within the *ab* plane, i.e., the *a*-axis length. However, except for this metric change, our low-temperature XRD measurements between 105 and 300 K show no other structural changes, e.g., of symmetry.

Magnetic susceptibility measurements reveal no anomaly around T^*. Starting from high-temperature χ_M values of ∼40 × 10^{-6} cm^3/mol, which are almost temperature independent in the range 100−350 K, the molar magnetic susceptibility increases to 0.003 cm^3/mol at 5 K. The observed paramagnetic contribution is attributed to a small contamination of the sample by magnetic impurities. The susceptibility data can be fitted to a modified Curie law, $\chi_M = C/T + \chi_o$, where the Curie term C/T accounts for the paramagnetic impurities; the temperature-independent part (χ_o) includes the diamagnetic contribution χ_{dia} from the closed electronic shells and the Pauli paramagnetic component χ_{Pauli} from the conduction electrons. The extrapolation of the data $1/T \rightarrow 0$ directly provides $\chi_o = -60(5) \times 10^{-6}$ cm^3/mol. After subtracting the core diamagnetism ($\chi_{dia} = -196 \times 10^{-6}$ cm^3/mol), the Pauli susceptibility of $\chi_{Pauli} \approx 135 \times 10^{-6}$ cm^3/mol is obtained for La_2TeI_2. The observed χ_{Pauli} is approximately two times larger than a value of 76 × 10^{-6} cm^3/mol, estimated from the band structure calculations according to $(\chi_{Pauli})_{calcd} = N(E_F)\mu^2_B$.[32]

Electronic Band Structure. La_2TeI_2 is isostructural and isovalence-electronic with the ternary zirconium halide Zr_2CCl_2, thus adopting general electronic features of the latter compound.[33] The electronic band structure and density of states (DOS) for La_2TeI_2 derived from the LDA calculations are shown in Figure 4. The bonding combinations of the I 5p states hybridized with the s and p states of lanthanum form the valence band manifold between −4 and −2 eV

(29) Pauling, L. *The Nature of the Chemical Bond*, 3rd ed.; Cornell University Press: Ithaca, NY, 1960.
(30) Wilson, J. A.; Di Salvo, F. J.; Mahajan, S. *Adv. Phys.* **1975**, *24*, 117.
(31) Schlenker, C.; Dumas, J.; Escribe-Filippini, C.; Guyot, H. In *Low dimensional properties of molybdenum bronzes and oxides*; Schlenker, C., Ed.; Kluwer Academic Publishers: Dordrecht, Boston, London, 1989.
(32) Ashcroft, N. W.; Mermin, N. D. *Solid State Physics*; Saunders College Publishing: Philadelphia, 1976.
(33) Ziebarth, R. P.; Hwu, S.-J.; Corbett J. D. *J. Am. Chem. Soc.* **1986**, *108*, 2594.

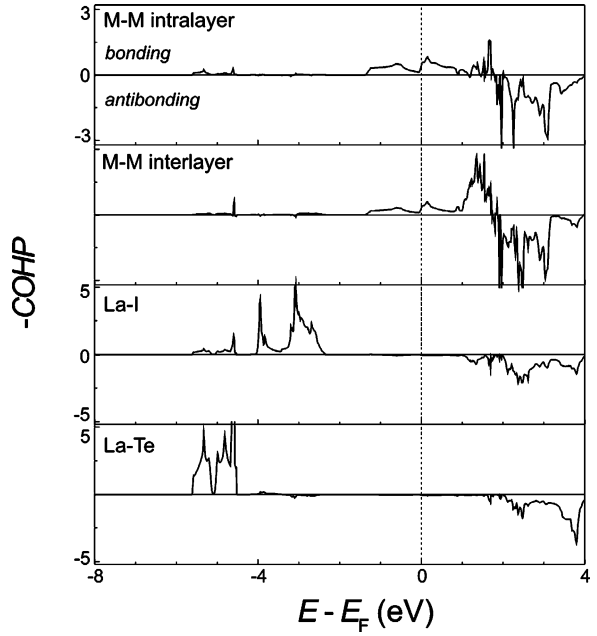

Figure 5. Crystal orbital Hamilton population (COHP) diagram of the La−La, La−I, and La−Te bonds in La_2TeI_2. The negative COHP values correspond to bonding interactions and the positive ones to antibonding interactions. The dashed line displays the position of the Fermi level.

relative to the Fermi level, E_F. The bands derived from tellurium 5p states lie at around −5 eV. The conduction band ($E > -2$ eV) is primarily comprised of the La 5d and 4f states (above E_F) with the predominant contribution of the d_{xy}, d_{yz}, and d_{z^2} orbitals to its bottom part. The Fermi level crosses the conduction band close to Γ, just below a high-density spike in the DOS which results from the degeneracy of the metal d bands at Γ and their weak dispersion, if any, along the Γ−Z direction. The DOS per formula unit at the Fermi level is $N(E_F) \cong 2.37$ states/(eV·f.u.).

To analyze the chemical bonding, the COHP curves have been calculated for several representative bonds in La_2TeI_2 (Figure 5). These show that the La−La interactions, both intralayer and interlayer, are bonding in nature. However, the bonding states are not completely filled up to the Fermi level E_F, indicating that the electron count is far from that of optimized La−La bonding. In this regard, the optimal overlap would be reached at $E - E_F \approx 1.0-1.5$ eV, e.g., by introducing extra valence electrons through cation intercalation between the halide layers. It is interesting to note that there are minor contributions of the La−La and La−I bonding components in the "tellurium" band. For comparison of bond strengths, we have analyzed integrated COHP values (ICOHP) of the intralayer and the interlayer La−La interactions. The shorter interlayer La−La distances of 4.41 Å have an ICOHP value of − 0.11 eV/bond, compared with one of − 0.08 eV/bond for the longer in-plane La−La distances of 4.51 Å. This relation indicates stronger interactions between the metal atoms along the c axis, being in line with the Pauling bond order parameters, see above.

Figure 6 displays the Fermi surface (FS) of La_2TeI_2 calculated for a single slab 1T-La_2TeI_2 structure within the hexagonal unit cell. It consists of two parts: hexagonal/triangular hole cylinders around the Γ = (0,0) and $K = (2a^*/3, 2b^*/3)$ points, respectively, and six cylinderlike electron pockets along the c^* direction, which lie between the Γ and K points. The electron FSs are strongly anisotropic in the c^* direction and squeezed along [−1 1 0]*, yielding flat regions with a nesting vector parallel to this direction. However, nesting is much weaker than in the case of layered transition metal compounds.

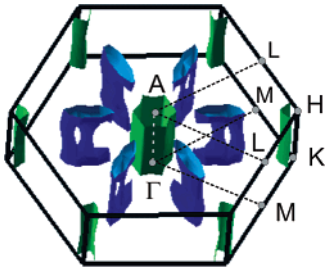

Figure 6. Fermi surface of a single La_2TeI_2 slab calculated in the hexagonal unit cell. The first Brillouin zone with characteristic high-symmetry points [Γ = (0,0,0), K = ($2\pi/3a$,$2\pi/3a$,0), M = (π/a,0,0), A = (0,0, π/c), H = ($2\pi/3a$,$2\pi/3a$, π/c), and L = (π/a,0, π/c)] is outlined.

According to band structure calculations performed with the structural parameters of La_2TeI_2 determined at 120 K, there are no significant changes neither in the electronic band structure nor in the Fermi surface except that the density of states at E_F decreases slightly from 2.37 to 2.35 states/(eV·f.u.) when compared with the room-temperature value.

Concluding Remarks

La_2TeI_2 can be prepared in high yields by a solid-state reaction of LaI_3, La, and Te in welded Ta ampoules filled with argon. Similar to other interstitial derivatives of the rare earth metal halides M_2ZX_2, the main structural feature of La_2TeI_2 is the presence of the metal atom double layers. Although the La−La distances (4.41−4.51 Å) are substantially larger than those found in binary layered metal-rich halides (3.93 Å for LaI,[34] 3.92 Å for LaI_2[35]), electronic band structure calculations and analysis of the COHPs indicate weak bonding within the metal atom framework, so that the system is expected to exhibit metallic yet strongly anisotropic transport properties. Indeed, La_2TeI_2 is metallic at room temperature, but exhibits a resistivity anomaly around 140 K. Such an electrical anomaly is frequently observed in layered transition metal chalcogenides with nested Fermi surfaces and associated with the formation of a charge density wave instability. Interestingly, the calculated Fermi surface for the title compound does contain small flat regions perpendicular to the [−1 1 0]* direction, which are however far from optimal nesting. It is striking that the a lattice parameter shows the same feature with temperature as seen in $\rho(T)$, indicating a close correlation between both. More detailed studies on single crystals of La_2TeI_2 will be necessary to better understand the origin of the unusual electrical properties found for this compound with a strongly anisotropic electronic structure.

(34) Martin, J. D.; Corbett, J. D. *Angew. Chem.* **1995**, *107*, 234−236; *Angew. Chem., Int. Ed. Engl.* **1995**, *34*, 233.
(35) Burrow, J. H.; Maule, C. H.; Strange, P.; Tothill, J. N.; Wilson, J. A. *J. Phys. C: Solid State Phys.* **1987**, *20*, 4115.

Acknowledgment. We gratefully thank G. Siegle for the electrical resistivity measurements and E. Brücher for the magnetic susceptibility measurements.

Supporting Information Available: Temperature-dependent magnetic susceptibility data, parameters of the TB-LMTO calculations, and LMTO band structure of La_2TeI_2 in the fat band representation showing contributions of selected La (s, p, and 5d) atomic orbitals. This material is available free of charge via the Internet at http://pubs.acs.org.

IC061675R